Optical assessment of head-mounted displays in visual space

Yonggang Ha and Jannick Rolland

The optics of head-mounted displays (HMDs) is designed from the pupil of the eye to the miniature display, and the optics is thus commonly solely assessed in the plane of the miniature display. Such assessment does not provide information that usefully interfaces with task-based performance metrics. We present a comprehensive framework for the assessment of the optics of HMDs in visual space, which applies to nonrotationally symmetric systems as well. Four key measures of visual performance are presented, and macro files were implemented to validate the framework. We illustrate the methods using an Erfle eyepiece. © 2002 Optical Society of America

OCIS codes: 110.3000, 120.3620, 220.4830, 080.1010, 330.4300.

1. Introduction

With the rapid development of virtual environment technology and wearable displays, the visual performance and human factor performance of head-mounted displays (HMDs) across multiple tasks are crucial. To this end, it is important to quantify the performance of the optics in visual space, given that visual metrics can then provide a baseline for usability and perception studies.[1]

The assessment of the design of HMDs in visual space is not customary because the optimization of the optical design is conventionally done from the location of the virtual image in visual space, where the stop is also located, to the miniature display. Such a layout allows one not only to equally handle collimated and noncollimated imaging during optimization without additional optics, but, most important, it ensures a sharp definition of the pupil location in object space, which facilitates the optimization process. However, because optimization is typically followed by an assessment in the same computational space, which is the miniature display space in this case, assessment in visual space is rarely provided.[2]

Assessment in visual space requires first flipping the optical system, so the lens can be ray traced backward. In the case of complex designs such as nonrotationally symmetric systems and systems with ill-defined pupils, flipping the optical system can be a challenge given that available functions do not provide a working solution. Full reentry of the system and additional controls such as pupil aiming may be required.[3] In addition, assessment in visual space requires computations based on the eye's visual acuity and depth of focus, itself a function of visual acuity and the size of the eye pupil. Perhaps because of the additional complexity these requirements bring, such computational capability is not typically provided in lens design software. One must resort to custom-written macros to compute performance in visual space, or, in some appropriate cases, one can also resort to estimate performance in visual space on the basis of known performance in display space and basic knowledge of the human visual system. In this paper the criteria presented for the assessment of the optics of HMD yield accurate performance directly in visual space, without approximations. The capability to perform exact computations rather than estimations is not only important but also efficient once macros are established.

2. Metrics in Visual Space

All computations in visual space require that the HMD optical system be flipped to allow backward ray tracing. This step is assumed in the description that follows. In this section we bring forth some generalized criteria for the assessment of the optics of HMDs in visual space, which are the modulation transfer function (MTF) in cycles/arc min, astigma-

The authors are with the School of Optics, Center for Research and Education in Optics and Lasers, University of Central Florida, Orlando, Florida 32816-2700. Y. Ha's e-mail address is ha@odalab.ucf.edu.

Received 22 October 2001; revised manuscript received 1 April 2002.

0003-6935/02/255282-08$15.00/0

Table 1. Three Steps to Compute the MTF in Visual Space

Step	Description
1	Insert a perfect lens in the exit pupil to bring the image into focus.
2	Set the correct focal length of the perfect lens to insure that 1 arc min maps to 1 mm on the image plane.
3	Compute the MTF on the image plane of the perfect lens.

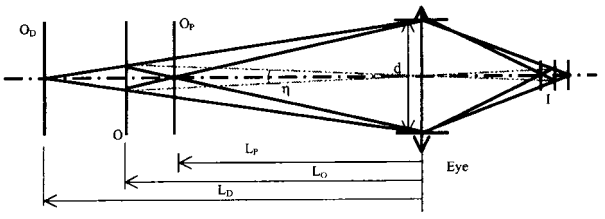

Fig. 1. Schematic layout of imaging of the eye and the corresponding depth of field. I, image of the eye lens; O, nominal object plane.

tism in both diopters and arcminutes, shift in accommodation (referred to as accommodation shift hereafter) in diopters, and transverse color smear in arcminutes. Distortion, which changes sign when a lens is ray traced backward, is invariant in magnitude across spaces when expressed in percentage.

A. Modulation Transfer Function

For MTF assessment, the unit of spatial frequency should be converted from cycles per millimeter into cycles per arcminute (cycles/arc min). Although such conversion can be estimated by a simple scaling factor, exact computation leads to different MTFs as a consequence of residual distortion as detailed in Section 3. So the difference in MTFs can be significant with increased distortion, which is often present and significant in HMD designs. If distortion is compensated for with preimage processing, the MTFs can be made equivalent. It is, however, rarely done in current systems.

The accurate computation of the MTF in cycles/arc min is composed of the following steps summarized in Table 1. On the surface of the exit pupil where the eye will be located, a perfect lens is inserted to bring the image into focus. In the case of MTF computation, the only requirement for the perfect lens is that the effective focal length f' is such that 1 arcminute maps to 1 mm on the image plane of the perfect lens. We shall see in Subsection 2.B that a perfect lens with a focal length approaching that of the human eye is required for other assessments. On the basis of the imaging equation for a thin lens in air,[4] the focal length f' can be computed as

$$f' = \frac{1}{\tan \theta - (1/L)}, \tag{1}$$

where θ equals 1 arc min and L is the virtual image distance of the HMD measured from the pupil of the eye. According to a sign convention in which positive distances go from left to right, L takes on a negative value in Eq. (1).[5] For the last step, we compute the MTF on the image plane of the perfect lens to yield directly the MTF in cycle/arc min.

B. Astigmatism and Accommodation Shift

Given a point in the field of view (FOV), astigmatism is measured as the difference in vergence between the sagittal and the tangential components of a small beam of light around the chief ray. The minimum resolution loss that is due to astigmatism can be defined by one choosing a focus plane one-half way between the sagittal and the tangential foci. In visual space this plane corresponds to an accommodation shift from the nominal virtual image plane. Accommodation shift is thus measured as the difference in vergence between the nominal virtual image point and the midpoint between the sagittal and the tangential images of that point.

When astigmatism is measured conventionally in the space of the miniature liquid-crystal display, astigmatism is measured either as the distance between the sagittal and the tangential foci in millimeters or as the length of the lines formed on the tangential or the sagittal surfaces in millimeters. In visual space, astigmatism is best evaluated in diopters for the longitudinal component or arcminutes for the transverse component. An object distance D_{Lm} expressed in diopters is defined as the inverse of the distance L_m expressed in meters. If the object is at infinity, D_{Lm} equals zero and the rays are collimated. D_{Lm} has a positive value when the object is in front of the eye or, equivalently, the light entering the eye pupil is divergent. If D_{Lm} is negative, the light entering the eye is convergent, and most people cannot bring the image into focus.

Given a virtual image presented in a HMD, objects can be perceived sharply around the nominal virtual screen distance where the eyes are focused, given the depth of focus and corresponding depth of field of the human visual system. Let us denote O_D and O_P as the distal and proximal planes that define the depth of field, L_D and L_P as the distances of these two planes from the eye, and L_O as the nominal focusing distance; all are represented in Fig. 1. The depth of field is determined by the visual acuity angle η, also shown in Fig. 1, and the diameter d of the eye pupil. The acuity angle η is defined either by the resolution in visual space as set by the angular subtends of a pixel or by the acuity of the human visual system. The former presents performance for a given display, and the latter provides additional information in terms of the potential performance of the optics to match visual acuity. It is important to assess the optics with respect to the acuity of the human visual system as well given that higher-resolution miniature displays are constantly becoming commercially available.

Table 2. Ten Steps to Compute Astigmatism and Accommodation Shift in Visual Space

Step	Description
1	Add a perfect lens with an aperture size equivalent to the pupil of the eye (depends on illumination) to bring the image into focus.
2	Trace rays and get the sagittal and tangential foci across the FOV.
3	Compute the sagittal and the tangential defocus values as well as their averages with respect to the paraxial image plane.
4	Convert all defocus values to diopters.
5	Compute the diopter range for the depth of field and eliminate the diopter values outside the depth of field.
6	Compute the difference between the sagittal and the tangential diopter values for astigmatism.
7	Compute the difference between the average diopter value and the nominal diopter value for accommodation shift.
8	Print 2D data tables of astigmatism and accommodation-shift values as a function of the FOV, and draw 2D plots accordingly.
9	Compute accommodation blur in arcminutes.
10	Print 2D data tables of accommodation blur in arcminutes as a function of the FOV, and draw a 2D plot accordingly, showing the residual blur greater than 1 arc min.
11	Compute astigmatism in arcminutes.
12	Print 2D data tables of astigmatism in arcminutes as a function of the FOV, and draw a 2D plot accordingly, showing astigmatism greater than 1 arcminute.

The larger η is, the larger the depth of field, but the lower the achievable resolution. The distances L_D and L_P expressed in diopters are given by

$$D_D = \frac{1}{-L_D} = -\frac{d + \eta L_O}{L_O d},$$
$$D_P = \frac{1}{-L_P} = -\frac{d - \eta L_O}{L_O d}, \quad (2)$$

where d and L_O are expressed in meters and η in radians. Objects outside the depth of field will be seen more blurred than at L_O unless the user refocuses, and optical aberrations that extend outside this range would contribute to a loss in resolution. This concept was used to develop multifocal planes HMDs.[6] The concept is employed in this paper to quantify the extent to which the design performance in visual space is within the tolerance of the visual system.

In visual space, astigmatism and accommodation shift across the FOV can be computed according to the steps summarized in Table 2. A perfect lens is added in the exit pupil where the eye will be located. The perfect lens should simulate an average human eye insofar as the focal length is concerned (i.e., $f' = 17$ mm). Furthermore, the size of the exit pupil should be set to a value corresponding to low levels of illumination (i.e., a 3-mm pupil diameter is employed in the computations presented hereafter). The pupil size and focal length together set the depth of focus and the corresponding depth of field of the human eye given by Eq. (2), which is utilized to set a tolerance on acceptable astigmatism and accommodation shift for the design. We then trace sagittal and tangential rays to the image plane of the perfect lens with a small aperture value (i.e., close skew rays) around the chief ray to obtain the focus locations of the sagittal and tangential rays across the FOV, respectively. With nonrotationally symmetric systems, rays in XZ and YZ sections are traced instead.[7,8] Also, the average values of the sagittal and tangential defocus values with respect to the paraxial image plane position are computed. The defocus values are expressed in diopters as follows:

$$D = -\left(\frac{1}{L' + \Delta} - \frac{1}{f'}\right), \quad (3)$$

where L' is the paraxial image distance behind the perfect lens, Δ is the defocus value for astigmatism or the average defocus value for accommodation shift, and f' is the focal length of the perfect lens.

The diopter values D that fall outside the depth of field are eliminated in the final graphical representation of the performance when dots are set at the respective points in the FOV. Other symbols can be used if such representation is not optimal, such as for off-axis designs in which the above-tolerance values do not automatically reside at the edge of the FOV. Results of the computation are presented as a two-dimensional (2D) data table of retained astigmatism and accommodation-shift values as a function of the FOV and as a 2D plot. To evaluate the blur caused by the accommodation-shift values that exceed the depth of field of the human visual system, we also present the size in arcminutes of blurred speckles across the FOV in both the 2D table and the plot. For this computation, the size of blurred spots are first calculated on the image plane of the perfect lens across the FOV, and the diameters of the spots are then converted into corresponding angular subtenses expressed in arcminutes in visual space. The computation of accommodation shift and accommodation blur should be consistent, where points that lie outside of the depth of field of the human visual system, and thus are missing in the plot of accommodation shift in diopters, appear as circles greater than 1 arc min in the plot of residual accommodation blur in arcminutes.

Although the assessment of astigmatism in diopters is quantitative and provides useful information for performance over the entire FOV, it can also be useful to know how elongated points in the FOV appear to the human eye. In this case, it is convenient to assess residual astigmatism on either the tangential or the sagittal surface on which points are imaged as lines. By definition, if the astigmatism values fall within the depth of field of the human visual system, the corresponding points will appear as sharp points and are represented as such. For values that exceed the depth of field of the human visual system, points

will appear as lines and are represented as such in units of arcminutes. The computation of astigmatism in both diopters and arcminutes should yield consistent results, where points that lie outside of the depth of field of the human visual system, and thus are missing in the plot of astigmatism in diopters, appear as lines greater than 1 arc min in the plot of astigmatism in arcminutes. This observation is validated in Section 3 of the paper.

C. Transverse Color Smear

For HMDs with color capability, transverse color smear can limit image quality and must be assessed. In visual space, transverse color smear will be measured in arcminutes. Two kinds of transverse chromatic aberration will be assessed: transverse lateral color and transverse secondary color. Transverse lateral color is the chief ray location difference of the two outer wavelengths measured in arcminutes over the FOV. For the visible spectrum the outer wavelengths are usually C and F. For those optical systems corrected in lateral color for C and F wavelengths, the residual chromatic smear is from secondary color, which is defined by the chief ray location difference of the reference wavelength and the common point of the two outer wavelengths. Thus transverse chromatic aberrations in visual space are computed according to the steps summarized in Table 3. Let us denote the coordinates of the chief rays of the outer wavelengths on the image plane as (X_C, Y_C) and (X_F, Y_F) and the coordinates of the chief ray for the reference wavelength as (X_R, Y_R). The transverse lateral color (TLC) and the transverse secondary color (TSC) expressed in arcminutes are computed by use of Eqs. (4) and (5) given by

$$\mathrm{TLC} = \left\{ \tan^{-1}\left[\frac{(X_C^{\,2} + Y_C^{\,2})^{1/2}}{L'}\right] - \tan^{-1}\left[\frac{(X_F^{\,2} + Y_F^{\,2})^{1/2}}{L'}\right]\right\} \times \frac{180(60)}{\pi}, \tag{4}$$

$$\mathrm{TSC} = \left(\tan^{-1}\left[\frac{(X_R^{\,2} + Y_R^{\,2})^{1/2}}{L'}\right] - \tan^{-1}\left\{\frac{\left[\left(\frac{X_C + X_F}{2}\right)^2 + \left(\frac{Y_C + Y_F}{2}\right)^2\right]^{1/2}}{L'}\right\}\right) \times \frac{180(60)}{\pi}, \tag{5}$$

where L' is the paraxial image distance. The results are similarly presented in the form of 2D data tables and 2D plots.

D. Other Considerations

For most HMDs, the designed exit pupil is much larger (e.g., 15 mm) than the size of the pupil of the human eye to allow for natural eye movements. Therefore, when the four key measures are assessed, it is necessary not only to reduce the pupil size to 3 or 4 mm but also to perform assessment for various values of decenter of the pupil of the eye within the full pupil of the HMD. To perform such analysis, it is sufficient to decenter the pupil and to compute performance by use of the same formalism. Presentation of the results as 2D plots instead of only as tables provides an effective tool for analysis, especially in the case of asymmetry.

Because HMDs are visual instruments, the photopic eye response to the whole visual spectrum could be taken into consideration for a more accurate analysis of the perceived transverse color smear. In such an approach, the wavelength weights could be adjusted to account for the relative luminous efficiency curves for the eye response, which falls either into the scotopic (dark-adapted vision) response or the photopic response, according to the illumination level specific to the application and the system.[9] Three equally weighted wavelengths were employed in this paper.

Table 3. Four Steps to Compute Transverse Color Smear in Visual Space

Step	Description
1	Add a perfect lens with appropriate aperture size to bring the image into focus.
2	Across the FOV, trace chief rays of the outer wavelengths and the reference wavelength to the image plane behind the perfect lens.
3	Compute transverse lateral color and transverse secondary color in visual space in terms of arcminutes on the basis of ray tracing.
4	Print 2D data tables of aberration versus FOV, and draw 2D plots accordingly.

3. Application of the Methods to an Erfle Eyepiece

To validate the framework presented, we implemented the methods detailed in this paper in several macro files written in this specific case, but with no loss of generality, with CODE V (software from Optical Research Associates, Pasadena, California). These macros are made accessible on the web at http://odalab.ucf.edu/macro and are written in ASCII format; therefore they are readable in any text editor and easily adaptable to any other macro language provided in other software. The various macros developed are listed in Table 4.

Because eyepiece optics is often employed in HMD designs, we chose an Erfle eyepiece as an example. An off-axis example assessed via an earlier version of the methods is provided by Rolland.[3] Table 5 provides the design specifications of the eyepiece, and Table 6 provides the optimized prescription data. The schematic design layout is provided in Fig. 2. To demonstrate the generalization of the assessment methods, we set different values of the FOVs in both the X and the Y directions.[7] Figures 3 and 4 show

Table 4. List of Available Macro Files at http://odalab.ucf.edu/macro

File name	Function
VSFlip.seq	Performs flip of optical systems, adds a perfect lens, and sets the pupil size to the user's request.
VSMTF.seq	Computes MTF as a function of spatial frequency in cycles per arcminute and output data table and plot.
VSTCS.seq	Computes transverse color smear in arcminutes, including transverse lateral color and secondary lateral color, and output data tables and plots.
VSACAS.seq	Computes accommodation shift and astigmatism in diopters and output data tables and plots.
AC2ARC.seq	Computes accommodation blur in arcminutes.
AST2ARC.seq	Computes astigmatism in arcminutes.

assessments of distortion and MTF evaluated on the liquid-crystal-display plane of the HMD. Figure 5 shows the layout of the optical system after flipping of the optics and insertion in the pupil of a perfect lens whose focal length, specified hereafter, depends on the assessment conducted.

Table 5. Design Specifications

Parameter	Specification
Object: Color liquid-crystal display	
a. Size	1.3-in. diagonal[a]
b. Active display area	Rectangular, 26.4 mm × 19.8 mm
c. Resolution	800 × 600 pixels
Eyepiece	
a. Type	Erfle eyepiece
b. Effective focal length	61.6 mm
c. Exit pupil diameter	10 mm
d. Virtual image distance	2 m from the eye pupil
e. Eye relief	25 mm
Other parameters	
Wavelength range	656 to 486 nm
FOV	30° in diagonal
Distortion	<5% over entire FOV

[a]1 in. = 2.54 cm.

Table 6. Prescription Data for the Erfle Eyepiece

Surface Number	Radii	Thickness	Glass
Object	Infinity	−2000.00	AIR
1 (Stop)	Infinity	26.55	AIR
2	−25.9	3.98	F2
3	−45.36	6.65	BK7
4	−29.64	0.50	AIR
5	2323.16	4.51	SSK1
6	−57.70	3.31	AIR
7	86.722	7.00	SK4
8	−35.57	2.50	SF12
9	343.63	60.30	AIR
Image	Infinity	0.00	

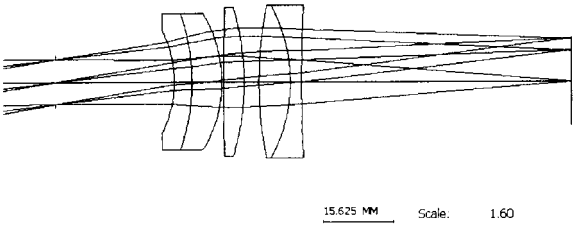

Fig. 2. Two-dimensional layout of the Erfle eyepiece.

To assess the MTF in visual space, we applied the macro file VSMTF.seq with the flipped system. On the basis of Eq. (1), the focal length of the perfect length at the stop surface is set to 1264.40 mm to yield the MTF with spatial frequency in units of cycles/arc min. It can be observed that the MTF expressed in cycles/arc min shown in Fig. 6 is similar in form to the MTF expressed in cycles/mm shown in Fig. 4. The two MTFs were purposely made equivalent in resolution, where we assumed 1-arc min resolution in visual space and an equivalent pixel size in display space. Yet they are not exactly the same because of the distortion of the system, which sets nonequivalent FOVs in object and image spaces. Therefore, although in the case presented the difference is small because distortion is small as shown in Fig. 3, the discrepancy can be significant for highly

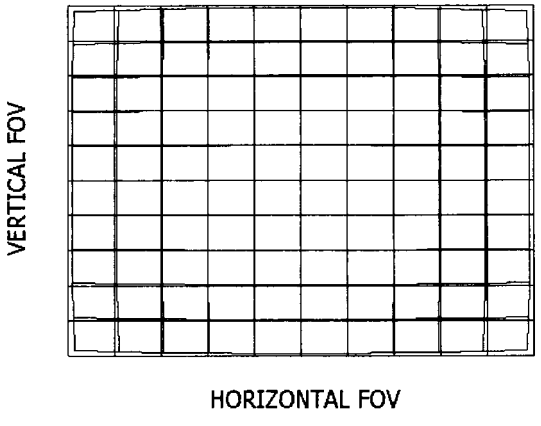

Fig. 3. Distortion of the Erfle eyepiece.

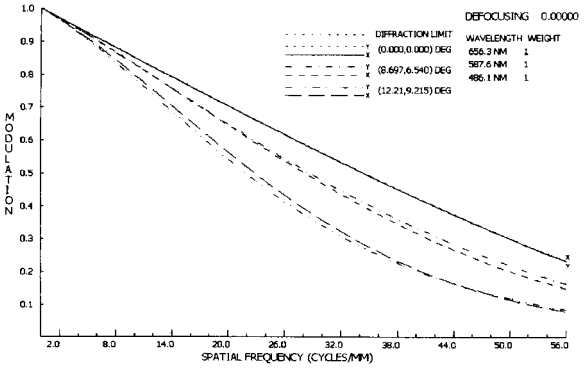

Fig. 4. Polychromatic MTF in cycles per millimeter with a 3-mm pupil.

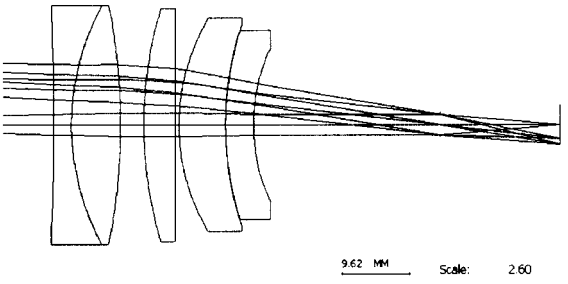

Fig. 5. Two-dimensional layout of the Erfle eyepiece after inversion and insertion of a perfect lens into the pupil.

distorted optics. It is thus preferable to accurately compute the performance in visual space as opposed to simply estimating it via a scaling factor of the MTF expressed in cycles/mm.

Accommodation shift and astigmatism in diopters were assessed with the macros VSACAS.seq. Accommodation blur and astigmatism in arcminutes were assessed with macros AC2ARC.seq and AST2ARC.seq, respectively. Given a 3-mm pupil and a resolution angle of 1 arc min, the depth of field ranges from 0.403 to 0.597 diopters. Accommodation shift expressed in diopters as a function of the FOV is shown in Fig. 7(a). Residual accommodation blur expressed in arcminutes as a function of the FOV is shown in Fig. 7(b). Astigmatism expressed in either diopters or arcminutes as a function of the FOV is shown in Figs. 8(a) and 8(b), respectively. The diameter of the circles in the plots is proportional to the magnitude of accommodation shift and astigmatism measured in diopters.

Results show that both accommodation shift and astigmatism are within the specified visual performance of the system for 80% of the FOV. Therefore all points within 80% of the FOV will be perceived as sharp points when the eyes accommodate in the plane of the virtual image provided. Other points are perceived on the tangential surface as lines as shown in Fig. 9. Furthermore, if the visual angle subtended by the pixels of the miniature display is larger than 1 arc min, the pixels will be resolvable and, in the case of residual astigmatism, will appear

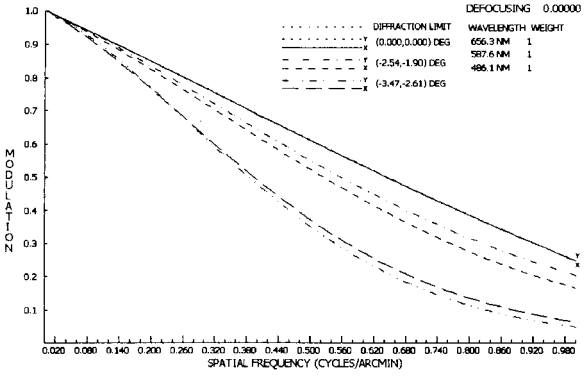

Fig. 6. Polychromatic MTF for a 3-mm pupil as a function of the spatial frequency in cycles per arcminute.

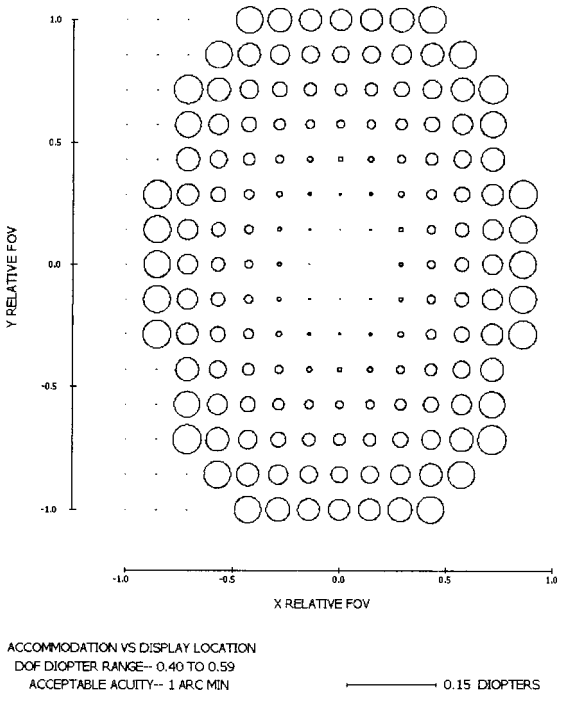

(a)

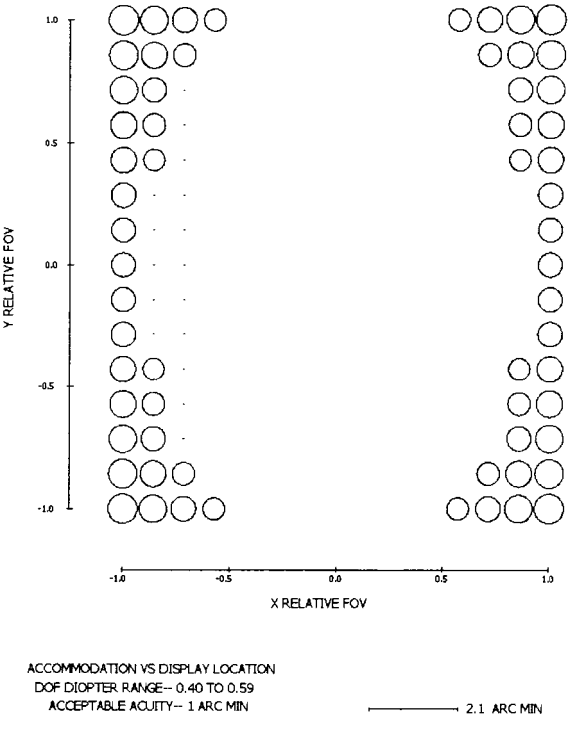

(b)

Fig. 7. (a) Accommodation shift in diopters for a centered 3-mm pupil. (b) Residual accommodation blur in arcminutes for a centered 3-mm pupil.

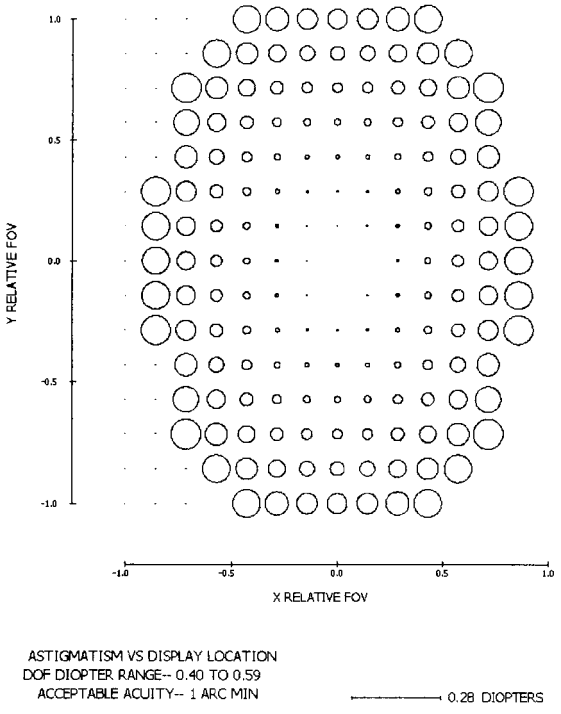

(a)

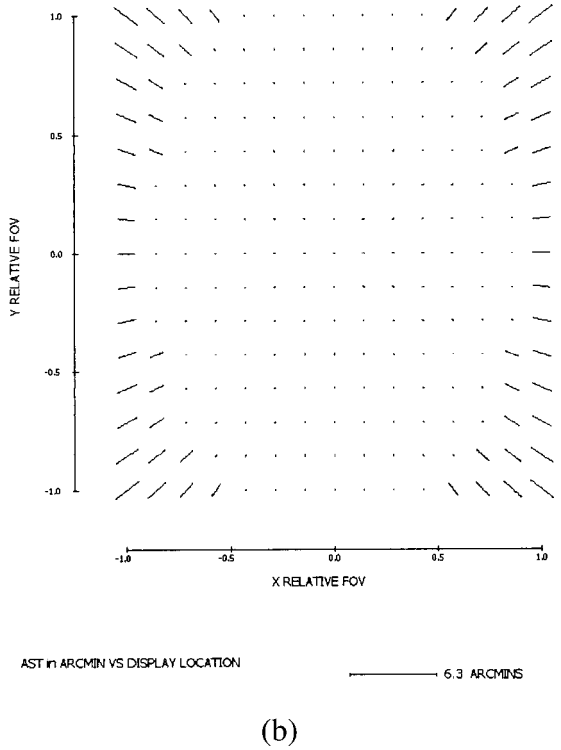

(b)

Fig. 8. Astigmatism in diopters for a centered 3-mm pupil. (b) Astigmatism in arcminutes for a centered 3-mm pupil.

elongated as well. Such a representation for astigmatism provides us with direct and quantitative information regarding the impact of astigmatism on the

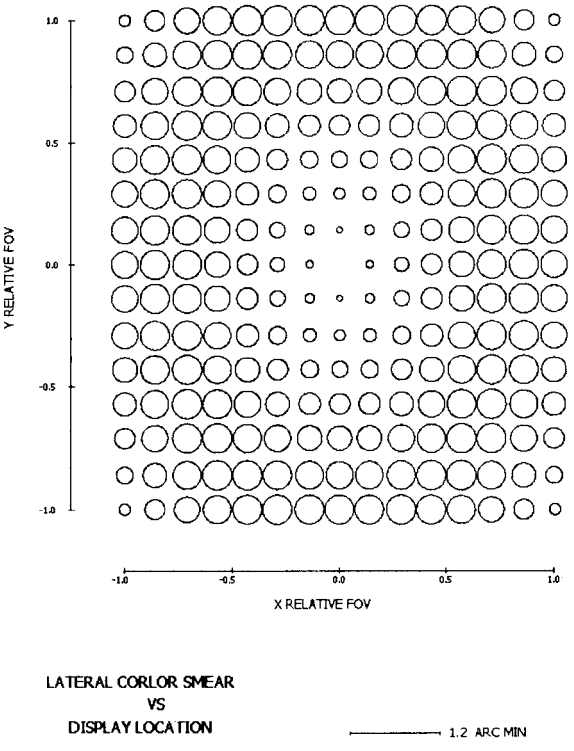

(a)

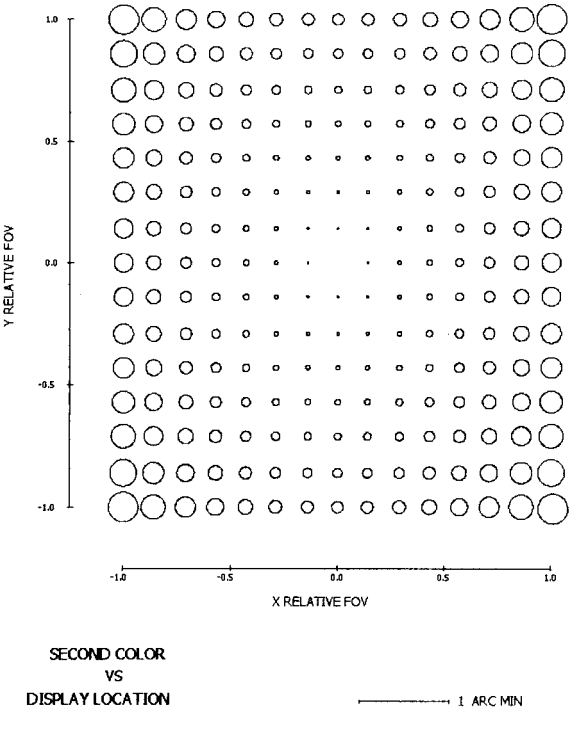

(b)

Fig. 9. (a) Transverse lateral color in arcminutes. (b) Transverse secondary color in arcminutes.

perception of points or objects in the FOV. As a comprehensive evaluation, we decentered the 3-mm eye pupil across the exit pupil of the eyepiece lens to investigate the effect of eye movement within the pupil on visual performance. Results, not reported here, clearly showed asymmetry of the accommodation shift and astigmatic plots across the FOV, yet results show that performance holds well across the FOV with eye motion.

Finally, applying the macro file VSTCS.seq to the flipped eyepiece, we computed the transverse lateral color and secondary color smear in arcminutes. Figure 9(a) shows the transverse lateral color versus FOV for a centered 3-mm pupil, and Fig. 9(b) provides the corresponding plot for secondary color smear. Results show that the design is not limited by either aberration given that all circles are less than 1 arc min, and therefore the color smear will not be resolved. This analysis can naturally be extended to decenters of the pupil.

4. Conclusion

The image quality in HMDs can be easily assessed in visual space. MTF performance is directly provided in cycles/arc min, accommodation shift in diopters, accommodation blur in arcminutes, astigmatism in both diopters and arcminutes, and transverse color smear in arcminutes. Assessment of HMD performance in visual space provides not only direct information about perceived image quality but also will surely help bridge the gap between optical design engineers and experts in the visual and human factor assessments of the technology.

We thank Martin Shenker for inspiring this research and Kevin Thompson and John Isenberg from Optical Research Associates for assistance with the development of some earlier version of the macro files provided here and some access to internal code related to computation of astigmatism line length, respectively. Finally, we thank Hong Hua for stimulating discussions about this research. This research is supported by National Institutes of Health–National Library of Medicine 1-R29-LM06322-01A1, the National Science Foundation IIS 00-82016 ITR and EIA-99-86051, and the Office of Naval Research–Virtual Technologies and Environments program.

References

1. J. P. Rolland, D. Ariely, and W. Gibson, "Towards quantifying depth and size perception in virtual environments," Presence Teleoper. Virtual Environments **4,** 24–49 (1995).
2. M. Shenker, "Image quality considerations for head-mounted displays," in *Digest of the International Optical Design Conference*, G. W. Forbes, ed. (Optical Society of America, Washington, D.C., 1994), pp. 334–338.
3. J. P. Rolland, "Wide-angle, off-axis, see-through head-mounted display," Opt. Eng. **39,** 1760–1767 (2000).
4. P. Mouroulis and J. Macdonald, *Geometrical Optics and Optical Design* (Oxford U. Press, New York, 1997).
5. J. P. Rolland, V. Shaoulov, and F. J. Gonzalez, "The art of back-of-the-envelope paraxial raytracing," IEEE Trans. Educ. **44,** 365–372 (2001).
6. J. P. Rolland, M. W. Krueger, and A. Goon, "Multifocal planes head-mounted displays," Appl. Opt. **39,** 3209–3215 (2000).
7. K. P. Thompson, "Aberration fields in nonsymmetric optical systems," Ph.D. dissertation, (University of Arizona, Tucson, Ariz., 1980).
8. J. R. Rogers, "Techniques and tools for obtaining symmetrical performance from tilted-component systems," Opt. Eng. **39,** 1776–1787 (2000).
9. P. Mouroulis, *Visual Instrumentation: Optical Design and Engineering Principles* (McGraw-Hill, New York, 1999).